Chemistry and Physics of Lipids 175–176 (2013) 9–19

Contents lists available at ScienceDirect

Chemistry and Physics of Lipids

journal homepage: www.elsevier.com/locate/chemphyslip

Thermodynamic and kinetic investigations of the release of oxidized phospholipids from lipid membranes and its effect on vascular integrity

Charles T.R. Heffern[a], Luka Pocivavsek[b,*], Anna A. Birukova[c], Nurgul Moldobaeva[c], Valery N. Bochkov[d], Ka Yee C. Lee[a,**], Konstantin G. Birukov[c,***]

[a] Department of Chemistry, University of Chicago, 929 E. 57th Street, Chicago, IL 60637, USA
[b] Department of Surgery, University of Pittsburgh Medical Center, 200 Lothrop Street F600, Pittsburgh, PA 15213, USA
[c] Section of Pulmonary and Critical Care, Department of Medicine, University of Chicago, 5841 S. Maryland Avenue, Chicago, IL 60637, USA
[d] Department of Vascular Biology and Thrombosis Research, Medical University of Vienna, Spitalgasse 23, 1090 Vienna, Austria

ARTICLE INFO

Article history:
Received 25 January 2013
Received in revised form 30 May 2013
Accepted 17 July 2013
Available online 30 July 2013

Keywords:
Oxidized phospholipid
Cell mechanics
Langmuir monolayer
Surface thermodynamics
Gibbs isotherm

ABSTRACT

The lipid membrane not only provides a rich interface with an array of receptor signaling complexes with which a cell communicates, but it also serves as a source of lipid derived bioactive molecules. In pathologic conditions of acute lung injury (ALI) associated with activation of oxidative stress, unsaturated phosphatidyl cholines overlooking a luminal space undergo oxidation leading to generation of fragmented phospholipids such as 1-palmitoyl-2-hydroxy-sn-glycero-3-phosphocholine (lysoPC), or 1-palmitoyl-2-arachidonoyl-sn-glycero-3-phosphocholine (PAPC) full length oxygenation products (oxPAPC). Using Langmuir monolayers as models of the lipid bilayer, we evaluated the propensity of these phospholipids to solubilize from the cell membrane. The results suggest that lysoPC is rapidly released as it is produced, while oxPAPC has a longer membrane bound lifetime. After being released from cell membranes, these oxidized phospholipids exhibit potent agonist-like effects on neighboring cells. Therefore, we correlate the presence of the two phospholipid groups with the onset and resolution of increased vascular leakiness associated with ALI through testing their effect on vascular endothelial barrier integrity. Our work shows that cells respond differently to these two groups of products of phosphatidyl choline oxidation. LysoPC disrupts cell–cell junctions and increases endothelial permeability while oxPAPC enhances endothelial barrier. These data suggest a model whereby rapid release of lysoPC results in onset of ALI associated vascular leak, and the release of a reserve of oxPAPC as oxidative stress subsides restores the vascular barrier properties.

1. Introduction

Oxidative stress is a cardinal feature of biological stress of various tissues. Increased production of reactive oxygen species and tissue oxidative stress has been described in many pathological conditions including acute respiratory distress syndrome, ventilator induced lung injury, chronic obstructive pulmonary disease, atherosclerosis, infection, and autoimmune diseases (Montuschi et al., 2000; Carpenter et al., 1998; Quinlan et al., 1996). As a result, oxidation of circulating and cell membrane phospholipids leads to generation of lipid oxidation products including esterified isoprostanes (Shanely et al., 2002; Lang et al., 2002) and lysophospholipids (Frey et al., 2000), which exhibit a wide spectrum of biological activities (Oskolkova et al., 2010). In particular, oxidized phospholipids exert prominent effects on lung vascular permeability, a hallmark feature of acute lung injury and pulmonary edema (Yan et al., 2005; Starosta et al., 2012). The presence of fragmented phospholipids (1-palmitoyl-2-hydroxy-sn-glycero-3-phosphatidyl choline (lysoPC), 1-palmitoyl-2-(5-oxovaleroyl)-sn-glycero-phosphatidyl choline, and 1-palmitoyl-2-glutaroyl-sn-glycero-phosphatidyl choline) as well as full length products of phosphatidyl choline oxidation (such as 1-palmitoyl-2-(5,6-epoxyisoprostane E2)-sn-glycero-3-phosphatidyl choline

Abbreviations: ALI, acute lung injury; lysoPC, 1-palmitoyl-2-hydroxy-sn-glycero-3-phosphocholine; PAPC, 1-palmitoyl-2-arachnidoyl-sn-glycero-3-phosphocholine; oxPAPC, full length PAPC oxygenation products; PEIPC, 1-palmitoyl-2-(5,6-epoxyisoprostane E2)-2n-glycero-3-phosphatidyl choline; DMPC, 1,2-dimyristoyl-sn-glycero-3-phosphocholine; EC, endothelial cells; TER, transendothelial electrical resistance; CMC, critical micelle concentration; PAH, PAF-acetyl hydrolase.

* Corresponding author. Tel.: +1 864 706 8258.
** Corresponding author. Tel.: +1 773 702 7068; fax: +1 773 702 0805.
*** Corresponding author. Tel.: +1 773 834 2636; fax: +1 773 834 2683.
E-mail addresses: pocivavsekl@upmc.edu (L. Pocivavsek), kayeelee@uchicago.edu (K.Y.C. Lee), kbirukov@medicine.bsd.uchicago.edu (K.G. Birukov).

0009-3084/$ – see front matter © 2013 Elsevier Ireland Ltd. All rights reserved.
http://dx.doi.org/10.1016/j.chemphyslip.2013.07.003

(PEIPC), or 1-palmitoyl-2-(5,6-epoxycyclopentenone)-sn-glycero-3-phosphocholine) has been detected by mass spectrometry analysis in the membranes of apoptotic cells, atherosclerotic vessels, and infected tissues (Huber et al., 2002; Kadl et al., 2004; Van Lenten et al., 2004; Subbanagounder et al., 2000; Watson et al., 1997).

To address the question of the dynamics of oxidized phospholipid release and its implications on lipid signaling, we have coupled a physical chemistry approach with a cellular study in the work presented here. Using a model membrane system, we examined how different chemical structures of various oxidized phospholipid species affect their stability within the membrane. Results obtained from this study have allowed us to propose a physical model based upon lipid surface thermodynamics to explain the potential origin of this differential release of oxidized lipids from a cell membrane. This model was further tested on endothelial cell monolayers, evaluating how different oxidatively modified phospholipid products affect cell monolayer integrity and barrier properties through paracrine signaling mechanisms. Finally, we are able to correlate our model of the release of oxidized lipids from a cell membrane to the natural progression of ALI based on the stability of different oxidized lipid species in the cell membrane and their effects on the barrier properties of endothelial cell monolayers.

2. Materials and methods

2.1. Materials

1–2-Dimyristoyl-*sn*-glycero-3-phosphocholine (DMPC) and lysoPC were obtained in powder form and 1-palmitoyl-2-arachidonoyl-*sn*-glycero-3-phosphocholine (PAPC) was obtained dissolved in chloroform at a concentration of 5.0 mg/ml from Avanti Polar Lipids (Alabaster, AL) and used without further purification. Lipids were stored at −20 °C in glass vials.

Oxidized 1-palmitoyl-2-arachidonoyl-sn-glycero-3-phosphocholine (oxPAPC) was obtained by exposure of dry PAPC to air as previously described (Watson et al., 1997; Birukov et al., 2004; Birukova et al., 2007). The extent of oxidation was measured by positive ion electrospray mass spectrometry described elsewhere (Watson et al., 1997). Oxidized lipids dissolved in chloroform were stored at −70 °C and used within 2 weeks after mass spectrometry testing. All oxidized and non-oxidized phospholipid preparations were analyzed by the limulus amebocyte assay (BioWhittaker, Frederick, MD) and shown negative for endotoxin.

Unless specified, all other biochemical reagents were obtained from Sigma (St. Louis, MO). Human pulmonary artery endothelial cells were obtained from Lonza Inc (Allendale, NJ), cultured according to manufacturers protocol, and used at passages 5–9. Solvents for Langmuir monolayers (chloroform and methanol) were obtained as HPLC grade from Fisher Scientific (Pittsburgh, PA).

Throughout the experiments, pure water (resistivity ≥ 18 MΩ cm) obtained from a Milli-Q UV Plus system (Millipore, Bedford, MA) or a Milli-Q Advantage A10 system was used as the subphase for Langmuir monolayer and Gibbs absorption experiments.

2.2. Langmuir monolayer and Gibbs adsorption experiments

To test the thermodynamic and kinetic stability of phospholipids in model cell membranes, Langmuir monolayer and Gibbs adsorption experiments were performed in a custom built Langmuir trough. Details of the Langmuir trough set-up have been discussed previously (Gopal and Lee, 2001; Pocivavsek et al., 2008a, b). Briefly, the setup consisted of a custom-made Teflon trough equipped with two Teflon barriers whose motions were precisely controlled by a pair of translational stages (UTM100, Newport, Irvine, CA) for symmetric compression or expansion of monolayers at the air/water interface. A fixed Wilhelmy balance (Riegler and Kirstein, Berlin, Germany) was used to measure interfacial surface pressure. Subphase temperature was maintained within 0.5 °C of the desired temperature of 37 °C with a homebuilt control station comprised of thermoelectric units (Marlow Industries, Dallas, TX) joined to a heat sink held at 20 °C by a Neslab RTE-100 water circulator (Portsmouth, NH). The entire assembly is mounted on a vibration isolation table (Newport, Irvine, CA) and controlled by a custom software interface written using LabView 6.1 (National Instruments, Dallas, TX).

Langmuir monolayer spreading solutions were prepared by dissolving DMPC and PAPC in chloroform and lysoPC in 90/10 chloroform/methanol at a concentration of 0.1 mg/ml. Spreading solutions of oxPAPC were prepared by diluting with chloroform to a concentration of 0.1 mg/ml.

Langmuir monolayers were spread at the air/water interface by gently depositing drops onto the surface and the organic solvent was allowed to evaporate for 20 minutes to allow for equilibration. All compressions were carried out with a linear speed of 0.1 mm/s and isotherm measurements in the form of surface pressure (mN/m) versus area per lipid molecule (nm^2/molecule) taken at one-second intervals.

For the constant area stability experiments, monolayers of lysoPC, oxPAPC, or DMPC were compressed to the target surface pressure of 5, 10, 15, 20, 25, 30, 35, or 40 mN/m, compression was then stopped and the surface pressure recorded as a function of time for 1000 s. For the constant pressure experiments, monolayers were again compressed to the above set of target pressures wherein the pressure was kept constant by continued compression as necessary using a custom feedback loop written into the motor control software. During the constant pressure loop the maximum compression speed was 0.01 mm/s. Initial rates of decay for the phospholipids were determined by averaging the rate of normalized area loss for the first 5 s after reaching the target surface pressure of 30 mN/m.

Gibbs adsorption experiments were carried out in the Langmuir trough. 2 ml stock solutions of lysoPC and oxPAPC were prepared in 90/10 H_2O/methanol; the solutions were then injected into 100 ml water subphase in the trough and surface pressure was monitored for one hour. The concentration of lipid in the 100 ml subphase was used in determining the critical micelle concentration.

2.3. Fitting of isotherms

The relative stability of the oxidized- and lyso-phospholipids was evaluated by the fit of their isotherms by a two-dimensional equation of state. A theoretical fit is generated using an osmotic two-dimensional equation of state:

$$\Pi = \frac{q.kT}{a_w} \times \ln\left[\frac{1 + a_w/(A - a_e)}{f}\right]$$

where f and q are effective surface activity coefficients (for most lipids $f \sim$ and $q \sim 1$–4 (Wolfe and Brockman, 1988)), a_e is the excluded area per lipid molecule (~0.4 nm^2 for phosphatidylcholine headgroups), and a_w is the partial area per water molecule (~0.09 nm^2) (Feng et al., 1994; Wolfe and Brockman, 1988; Marsh, 1996).

2.4. Morphological analysis of endothelial monolayer integrity by immunofluorescence staining

The physiological effect of the release of the oxidized- and lyso-phospholipids in cases of ALI was assessed by visualizing monolayers of endothelial cells exposed to various concentrations

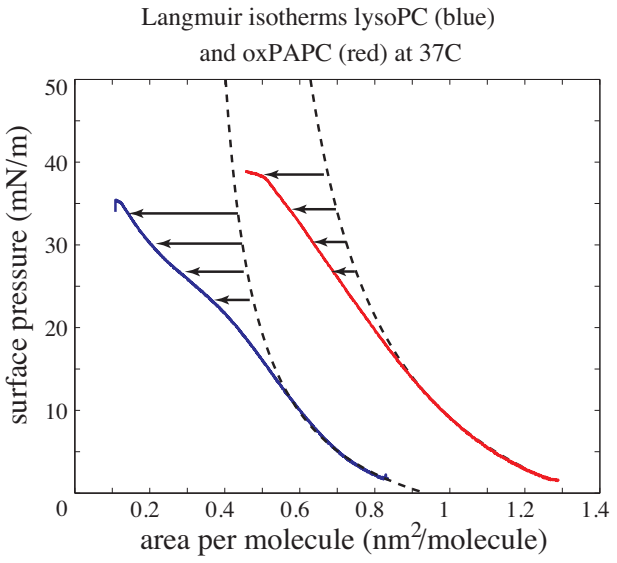

Fig. 1. Langmuir isotherms for lysoPC (blue) and oxPAPC (red) at 37 °C. Dashed black curves are theoretical fits using an osmotic-type surface equation of state: $\Pi_{\text{lysoPC}} = 54\ln(1 + 0.1/(A - 0.35)/1.171)$ and $\Pi_{\text{oxPAPC}} = 157\ln(1 + 0.091/(A - 0.45)/1.1)$. At higher surface pressures, both lipids deviate from the theoretical isotherms with lysoPC departing more strongly with further compression. These deviations represent surface relaxations not accounted for by the equation of state; as subsequent data show, the relaxation is due to desorption of lysoPC and oxPAPC molecules from the Langmuir monolayer into the subphase, with lysoPC desorbing faster than oxPAPC. (For interpretation of the references to color in this figure legend, the reader is referred to the web version of the article.)

of the phospholipids. Endothelial monolayers plated on glass cover slips were subjected to immunofluorescence staining with appropriate antibody, as described previously (Birukov et al., 2004). Texas Red phalloidin (Molecular Probes, Eugene, OR) was used to visualize F-actin, and antibody to VE-cadherin (Santa Cruz, CA) followed by staining with Alexa Fluor 488-labeled secondary antibody (Molecular Probes, Eugene, OR) was used to visualize cell–cell adherens junctions. After immunostaining, slides were analyzed using a Nikon video imaging system (Nikon Instech Co., Tokyo, Japan). Images were processed with Adobe Photoshop 7.0 (Adobe Systems, San Jose, CA) software.

2.5. Measurement of transendothelial electrical resistance

To quantify the effects of oxidized phospholipids on the permeability of endothelial monolayers, transendothelial electrical resistance experiments were performed. Endothelial cells (EC) were grown to confluence in polycarbonate wells containing evaporated gold microelectrodes (surface area, 103 cm^2) in series with a large gold counter electrode (1 cm^2) connected to a phase-sensitive lock-in amplifier. The size of the small gold electrode is critical so that the impedance resulting from the presence of cells on the electrode will predominate over the resistance of the medium. Measurements of transmonolayer electrical resistance were performed using an electrical cell-substrate impedance sensing system (Applied BioPhysics Inc., New York, USA). Briefly, current was applied across the electrodes by a 4000-Hz AC voltage source with amplitude of 1 V in series with a 1 MΩ resistance to approximate a constant current source 1 μA. The in-phase and out-of-phase voltages between the electrodes were monitored in real time with the lock-in amplifier and subsequently converted to scalar measurements of transmonolayer impedance, of which resistance was the primary focus. These methods have been demonstrated to be a highly sensitive biophysical assay that indicates the state of cell

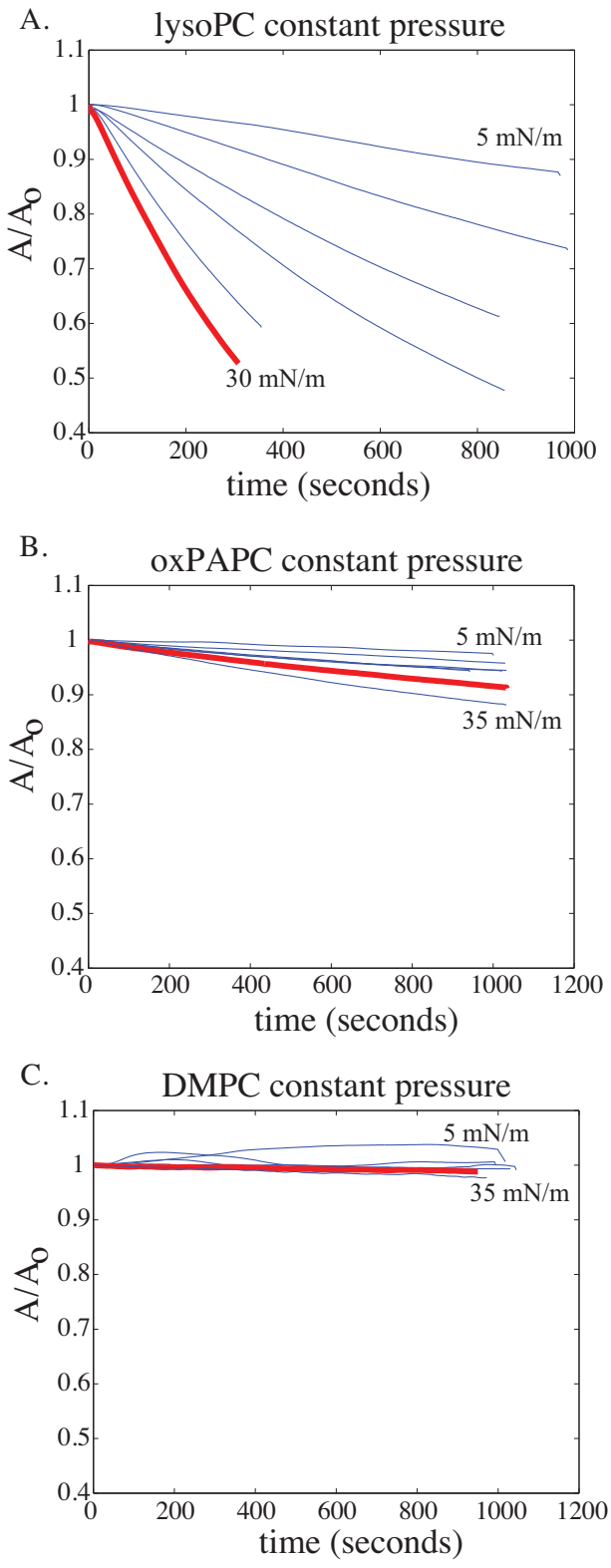

Fig. 2. Constant pressure stability curves for Langmuir monolayers of lysoPC (A), oxPAPC (B), and DMPC (C) at 37 °C. Plotted are the normalized area per molecule (A/A_0) as a function of time, where $A_0 = A(t = 0)$. The starting pressure is 5 mN/m and is increased in increments of 5 mN/m. The solid red curve represents the data for a surface pressure of 30 mN/m. DMPC shows no desorption up to 35 mN/m, as indicated by the horizontal nature of its A/A_0 curves even at bilayer equivalent pressures. LysoPC in contrast shows strong deviation from $A/A_0 = 1$ with increasing surface pressure indicating increasing desorption of lysoPC from the Langmuir film into the subphase. oxPAPC shows some desorption at all surface pressures but on a much slower time scale than lysoPC. (For interpretation of the references to color in this figure legend, the reader is referred to the web version of the article.)

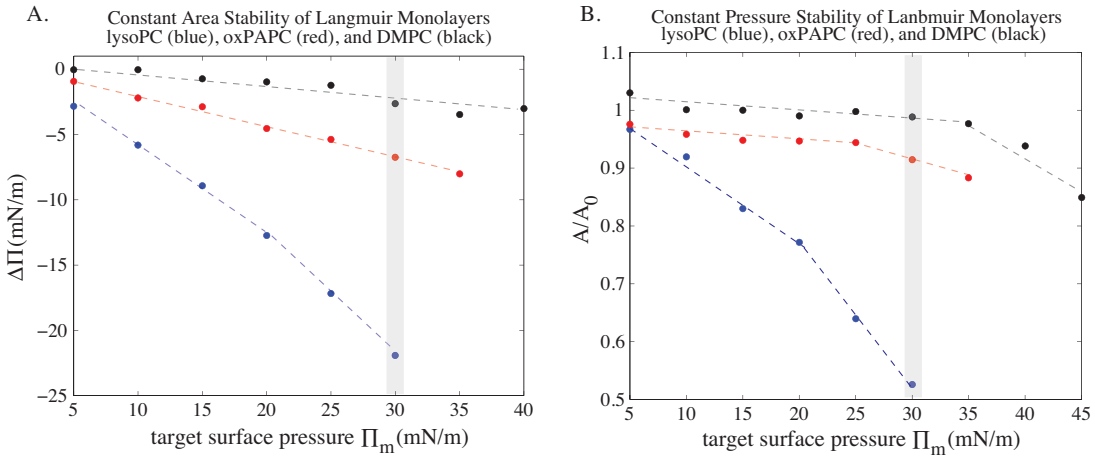

Fig. 3. Constant area (A) and constant pressure (B) stability diagrams of lysoPC (blue), oxPAPC (red), and DMPC (black) at 37 °C. The *y*-axis in (A) represents the drop in pressure occurring over 1000 s beginning from the initial target surface pressure (Π_m) to which the Langmuir monolayer was compressed before the monolayer was allowed to relax at constant area. DMPC is capable of maintaining target pressures to within a few mN/m far beyond bilayer equivalent pressures (shaded in gray is pressure where $\gamma_{phob}^{membrance} \sim \Pi_m$). lysoPC monolayers are unstable at all pressures but become increasingly so as the target pressure increases. oxPAPC shows intermediate stability, being closer to DMPC than lysoPC. The constant pressure diagram (B) compiles the data presented (using $A(t = \text{endpoint})/A_0$) and shows a similar stability trend as the constant area plot: DMPC ≥ oxPAPC ≫ lysoPC. (For interpretation of the references to color in this figure legend, the reader is referred to the web version of the article.)

shape and focal adhesion (Giaever and Keese, 1993; Tiruppathi et al., 1992). The culture medium was replaced to basal media containing 2% fetal bovine serum; transendothelial electrical resistance (TER) was monitored for a steady state to be achieved and started again for 30 min to establish a baseline resistance (R_0). Agonist-mediated permeability was evaluated by measurement of TER (Birukova et al., 2007; Nonas et al., 2006).

3. Results

3.1. Langmuir monolayer and Gibbs adsorption experiments

In the absence of surface relaxations, whether they are in-plane phase transitions or out-of-plane through surface desorption, Langmuir isotherms of phospholipids are well characterized by

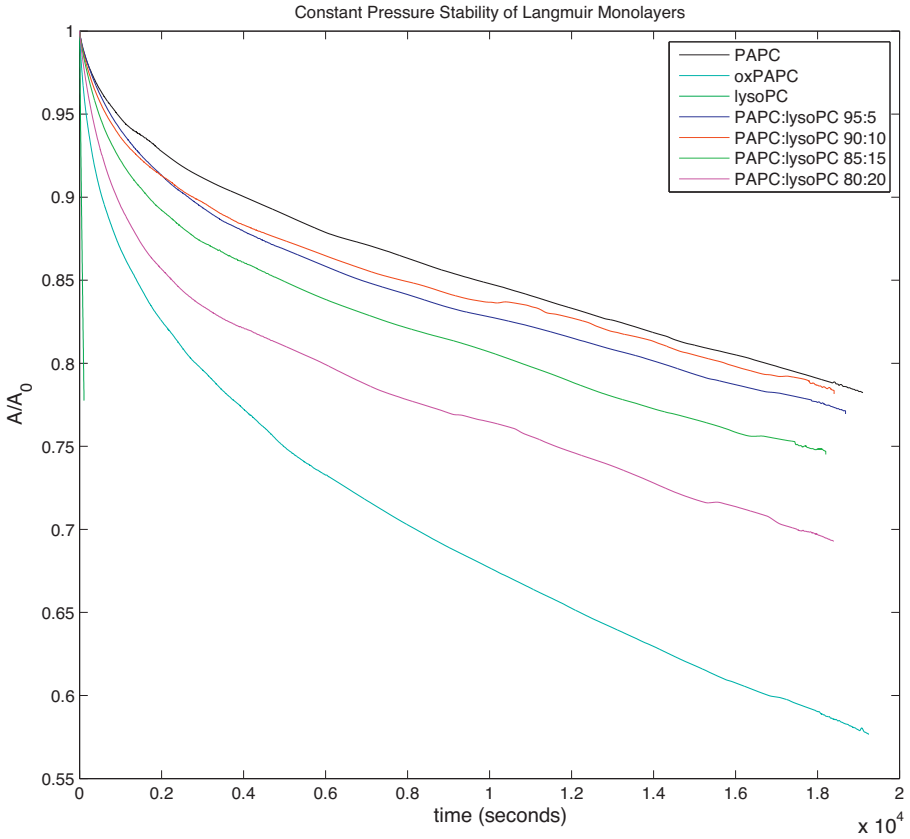

Fig. 4. Constant pressure stability curves for Langmuir monolayers of PAPC, lysoPC, oxPAPC, and mixtures of PAPC and lysoPC at 37 °C under bilayer equivalence pressure (30 mN/m). Plotted are the normalized area per molecule (A/A_0) as a function of time, where $A_0 = A(t = 0)$. The PAPC–lysoPC mixture curves maintain a consistent shape, except for an increasing offset in normalized area with the increasing concentration of lysoPC. The pure lysoPC stability curve is limited to short times due to the rapid solubilization of lysoPC from the interface as the membrane is compressed to the bilayer equivalence pressure.

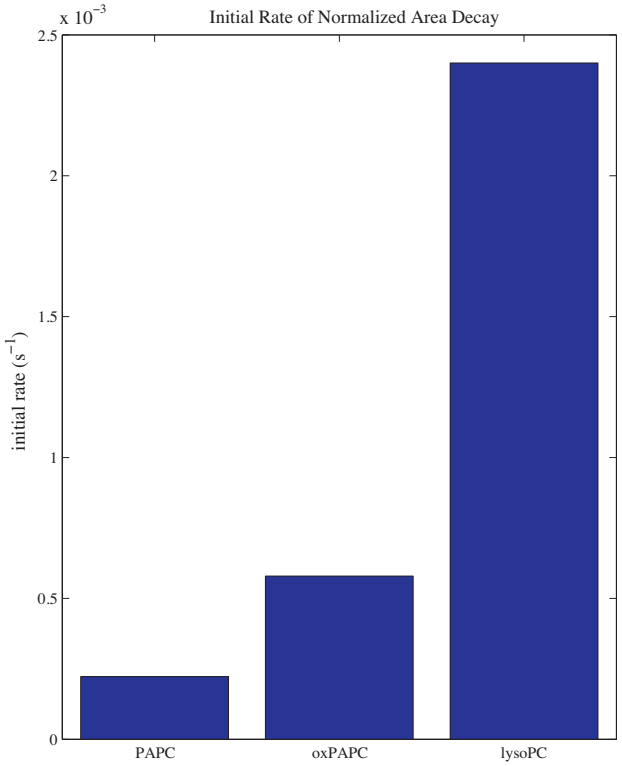

Fig. 5. Initial rate of normalized area per molecule (A/A_0) decay of pure PAPC, oxPAPC, and lysoPC at the bilayer equivalence pressure (30 mN/m). lysoPC exhibits a rate of area decay due to solubilization into the bulk phase ~10× greater than the rate of PAPC and ~5× greater than the rate of oxPAPC.

two-dimensional equations of state. The isotherms of two oxidized natural phospholipids, lysoPC, a fragmented phospholipid product of PAPC, and oxPAPC, a full length oxidized product of PAPC, are well characterized by an osmotic two-dimensional equation of state at surface pressures below 15 mN/m; however, at higher surface pressures the isotherms for both oxidized products move to a lower area per molecule than what would be expected for a fully liquid expanded monolayer. The deviation is more pronounced for lysoPC than for oxPAPC (Fig. 1). To evaluate the stability of lysoPC and oxPAPC monolayers at different surface pressures, constant area and constant surface pressure experiments were performed.

Figs. 2 and 3B show the constant pressure experiments done with lysoPC, oxPAPC, and DMPC. DMPC (Fig. 2C) is used as a model saturated PC lipid and remains completely on the surface up to 35 mN/m, as shown by the lack of deviation of the normalized area curves from $A/A_0 = 1$. The lysoPC monolayer (Fig. 2A), on the other hand, is unstable at every surface pressure, as indicated by the increasing slope of the area curves. The data clearly show that lysoPC becomes increasingly unstable to desorption from the surface as the surface pressure increases. In other words, the lysoPC molecules leave the surface monolayer and dissolve into the subphase at faster rates as the surface pressure approaches 30 mN/m (the bilayer equivalent pressure). oxPAPC does desorb with increasing pressure (Fig. 2B), but at much slower rates than lysoPC. At a constant pressure of 30 mN/m, lysoPC loses half the molecules on the surface into the bulk subphase within 300 s, while oxPAPC loses only 10% in 900 s. Fig. 3A shows the compiled data for constant area stability experiments using lysoPC, oxPAPC, and DMPC. The surface stability at constant area trends that of the constant pressure experiments: DMPC ≫ oxPAPC ≫ lysoPC.

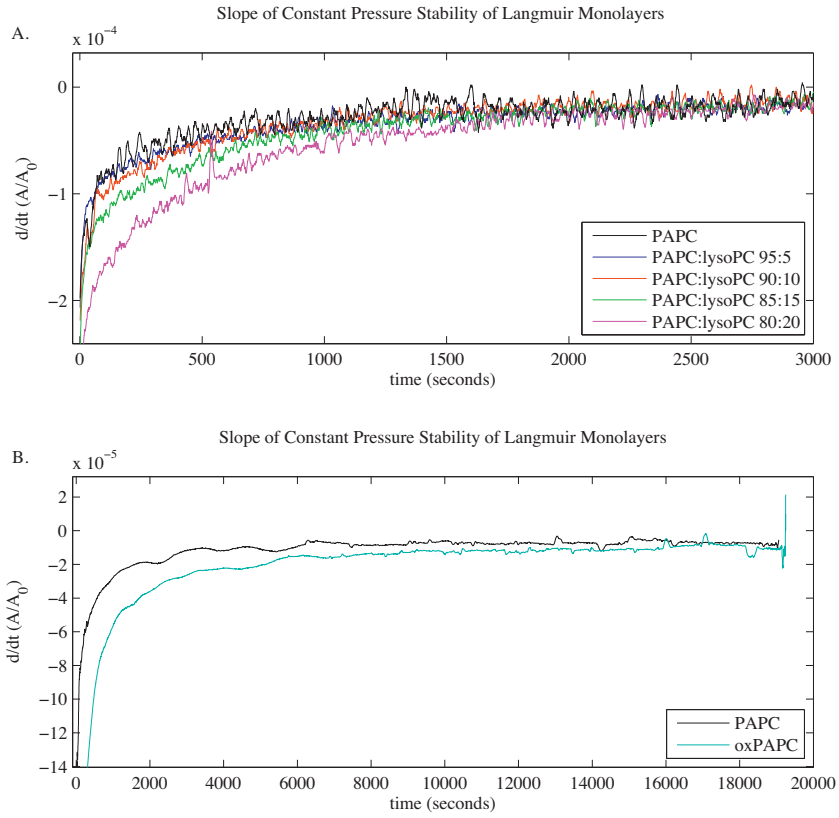

Fig. 6. Time derivative of the normalized area per molecule ($d/dt(A/A_0)$) vs. time plots of Langmuir monolayers of PAPC, lysoPC–PAPC mixtures (A), and oxPAPC (B) at 37 °C and the bilayer equivalence pressure (30 mN/m). The initial rate of area decay increases with increasing concentration of lysoPC. After ~2000 s, the rate of area decay for all mixtures relaxes to the rate of pure PAPC. oxPAPC maintains a rate of normalized area decay greater than the rate of pure PAPC for greater than 18,000 s.

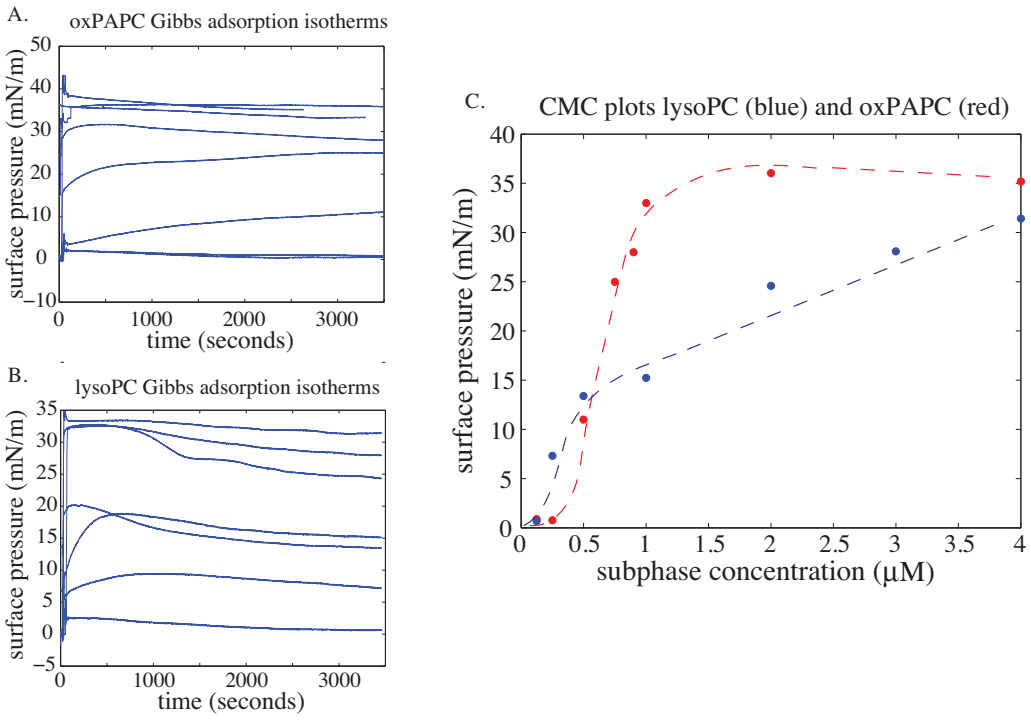

Fig. 7. Gibbs adsorption isotherms at 37 °C for oxPAPC (A) with bulk concentrations of 0.125, 0.25, 0.5, 0.75, 0.9, 1.0, 2.0, and 4.0 μM (increasing final pressure with increasing bulk concentration); and, lysoPC (B) with bulk concentrations of 0.125, 0.25, 0.5, 1.0, 2.0, 3.0, and 4.0 μM. In (C), the final surface pressure (taken at the end of an hour) is plotted against the bulk lipid concentrations generating a critical micelle concentration diagram. oxPAPC behaves like a strongly surface active molecule with a sharp increase in surface pressure over a narrow concentration regime (0.5–1 μM); lysoPC shows a broader transition spanning several μM, which is indicative of poorly surface active molecules.

Our next step was to determine the kinetics of phospholipid release from a model cell membrane using constant pressure experiments performed at 30 mN/m with mixtures of PAPC, lysoPC, and oxPAPC (Fig. 4). The initial rate of decay of the pure components (Fig. 5) indicates that lysoPC solubilizes out of the monolayer more rapidly than oxPAPC, and that the model membrane lipid (PAPC) is the most stable in the monolayer. The slope of the relative area curves of the mixtures of PAPC and lysoPC (Fig. 6A) shows that at short times, the behavior of the membrane is affected by the presence of lysoPC, but after ~2000 s, all of the lysoPC has been solubilized from the monolayer and the rate of the relative area decay collapses onto that of a pure PAPC monolayer. On the other hand, the slope of the relative area curve of oxPAPC shows a rate of decay greater than that of the PAPC–lysoPC mixtures for greater than 18,000 s (Fig. 6B).

To quantitate the hydrophobicity and surface activity of lysoPC and the oxPAPC mixture, Gibbs adsorption experiments were performed (Fig. 7A and B). Critical micelle concentrations (CMC) for the two systems were determined by plotting the equilibrium surface pressure of the lipid solution versus the bulk lipid concentration (Fig. 7C). LysoPC showed a gradual rise in surface pressure as the subphase lysoPC concentration increased from 0.5 to 4 μM; at the higher concentration limit, the surface pressure attained approached that of lysoPC collapse. oxPAPC showed a much sharper transition in surface activity over the narrower oxPAPC concentration range of 0.5–1 μM. The transition ranges over which the surface activity of the corresponding lipids increases define their respective CMC values.

To make the connection between our results obtained from model lipid systems to the biological manifestations of ALI and other forms of increased lung stress, we next analyzed whether the increased concentration of oxidized phospholipids played a role in initiating or resolving vascular leak. The effects of these oxidized phospholipids on endothelial monolayer integrity and endothelial permeability were evaluated in the following studies.

3.2. *Effects of different groups of oxidized phospholipids on endothelial monolayer integrity*

Monolayers of pulmonary endothelial cells were visualized with immunofluorescence staining to visualize cell–cell contacts and the cellular actin network to assess the effects of oxidized phospholipids on endothelial monolayer integrity and endothelial permeability. Non-treated pulmonary EC monolayers showed random distribution of actin filaments (red) and continuous line of VE-cadherin-positive (green) cell–cell contacts reflecting basal maintenance of monolayer integrity (Fig. 8A). Treatment with oxPAPC alone caused robust enhancement of cortical actin cytoskeleton, and prominent increase in VE-cadherin positive areas at the regions of cell–cell interface leading to tightening of EC monolayer and enhancement of EC barrier properties (Fig. 8B). By

Fig. 8. Effect of lyso-PC, oxPAPC and their combination on pulmonary endothelial cell cytoskeleton and monolayer integrity. Human pulmonary EC monolayers were left untreated (A); stimulated for 30 min with 20 μg/ml oxPAPC (B); 10 μg/ml lysoPC (C); or cotreated with 10 μg/ml lysoPC and 20 μg/ml oxPAPC (D). Analysis of actin cytoskeletal remodeling was performed by immunofluorescent staining with Texas Red phalloidin (red). Adherens junctions were detected by staining with VE-cadherin (green). Right panels show merged images of F-actin and VE-cadherin staining. Insets (E) depict higher magnification images with details of actin and adherens junction structures in control, lysoPC and oxPAPC stimulated cells. (For interpretation of the references to color in this figure legend, the reader is referred to the web version of the article.)

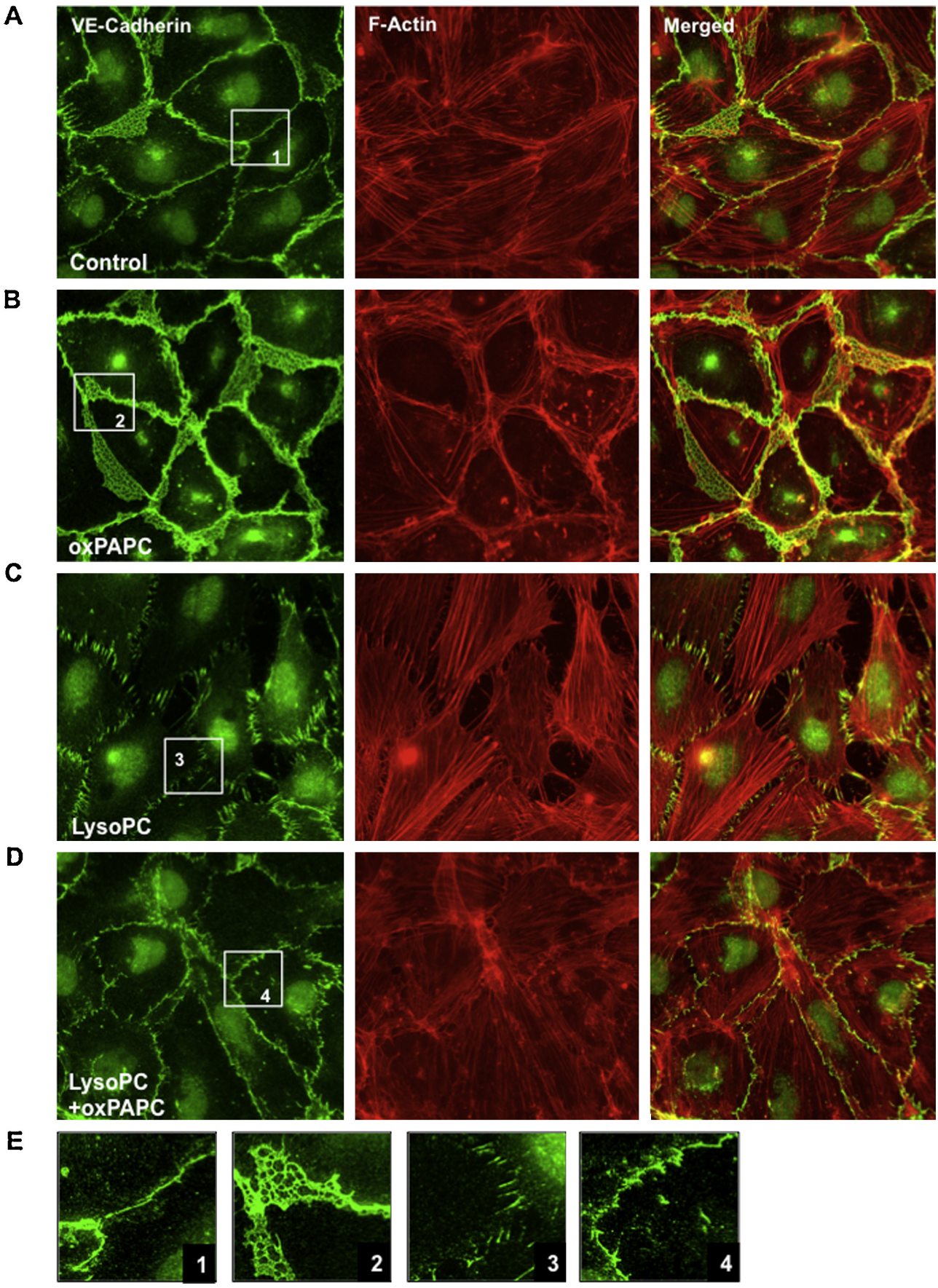
A
VE-Cadherin
F-Actin
Merged
1
Control
B
2
oxPAPC
C
3
LysoPC
D
4
LysoPC
+oxPAPC
E
1
2
3
4

contrast, treatment with lysoPC caused formation of actin stress fibers and disruption of continuous line of VE-cadherin at cell periphery reflecting endothelial monolayer disruption (Fig. 8C). Disruption of cell–cell junctions caused by lysoPC was attenuated by co-treatment with oxPAPC (Fig. 8D).

3.3. *Effects of different groups of oxidized phospholipids on endothelial permeability*

To quantitatively analyze the amount of endothelium disruption or protection caused by exposure to the oxidized phospholipids, TER measurements were made on endothelial monolayers treated with oxPAPC or lysoPC. Treatment of human pulmonary EC monolayers with 5–20 μg/ml of oxPAPC induced a sustained increase in TER, while further increase in oxPAPC concentration (50–100 μg/ml) caused acute and sustained TER decrease (Fig. 9A). These results are consistent with our previous findings (Birukov et al., 2004; Birukova et al., 2007; Starosta et al., 2012). In contrast to oxPAPC, treatment with fragmented phospholipid lysoPC failed to induce barrier protective effects at any concentration used. Instead, lysoPC caused EC barrier compromise in a dose-dependent manner (Fig. 9B), consistent with previous studies (Yan et al., 2005).

The EC barrier effects of lysoPC and oxPAPC were further examined through co-treatment of EC monolayers with both forms of oxidized phospholipid to determine whether the barrier disruptive effects of fragmented phospholipids can be reversed by the presence of barrier protective concentrations of oxPAPC. The co-treatment with fragmented phospholipids and full-length oxidation products indeed showed that the presence of oxPAPC attenuated the barrier-disruptive effects of lysoPC on EC monolayers (Fig. 9C).

4. Discussion

Acute lung injury is associated with massive oxidative stress leading to non-enzymatic phospholipid oxidation that generates oxygenated and fragmented phospholipid species (Bochkov et al., 2010; Lang et al., 2002). ALI-associated lysophospholipid production may be additionally stimulated by membrane-bound phospholipases (Munoz et al., 2006) that become activated under these conditions (Munoz et al., 2009), and may lead to increased accumulation of fragmented phospholipids in circulation as well as within cell membranes. Increased circulating levels of fragmented phospholipids act on lung endothelial cells and further promote lung inflammation and lung endothelial barrier disruption (Qiao et al., 2006).

Our study shows that lysophospholipids, representing the products of advanced phosphatidylcholine oxidation, release from lipid monolayers early, while release of full-length oxygenated phosphatidylcholine products is delayed. Although both species are products of phosphatidylcholine oxidation, their chemical structures clearly play an important role in determining their membrane stability: full-length oxygenated PAPC products such as PEIPC show decreased stability within the cellular membrane, yet are more membrane stable than fragmented phospholipids such as lysoPC. Interestingly, these oxidatively modified phospholipid products not only differ from each other in terms of membrane stability, but they also exhibit opposing effects on endothelial cell monolayer integrity and barrier properties through paracrine signaling mechanisms, with full-length oxygenated PAPC products showing barrier protective effects while fragmented phospholipids are highly barrier disruptive. These findings lead us to hypothesize that the acute phase of barrier dysfunction in ALI in vivo is dominated by high levels of fragmented phospholipids while barrier recovery is

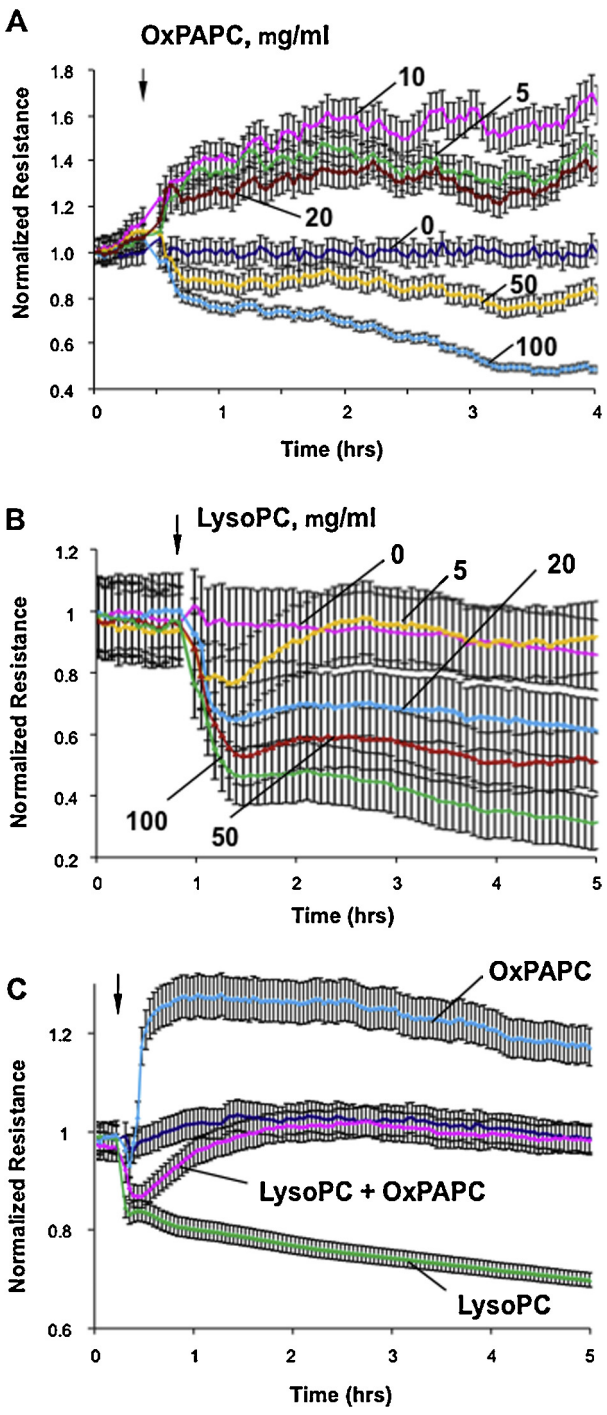

Fig. 9. Effects of OxPAPC, lyso-PC and their combination on endothelial monolayer permeability. Human pulmonary artery endothelial cells were grown on golden microelectrodes. At the time point indicated by arrow, cells were treated with: (A) 5 μg/ml, 10 μg/ml, 20 μg/ml, 50 μg/ml, or 100 μg/ml OxPAPC; (B) 5 μg/ml, 20 μg/ml, 50 μg/ml, or 100 μg/ml of lyso-PC; or (C) combination of 20 μg/ml OxPAPC and 20 μg/ml of lyso-PC followed by measurements of transendothelial electrical resistance (TER) reflecting EC monolayer barrier properties. Shown are representative results of five independent experiments.

associated with a delayed release of oxygenated full length PC with barrier enhancing properties.

The Langmuir and Gibbs monolayer experiments carried out with lysoPC and oxPAPC were designed to probe the surface thermodynamics and kinetics of these lipids. Unperturbed, a lipid bilayer (cell plasma membrane) is in mechanical equilibrium

implying a minimum in the total bilayer surface free energy (Marsh, 1996):

$$F_b \sim \psi_{phob} + \psi_{hyd} + \psi_{int} + \psi_{m\text{-}m} \quad (1)$$

where the terms represent the lipid hydrophobic, hydration, internal, and monolayer–monolayer coupling components, respectively. Physicochemically, the magnitude of the hydrophobic term is determined by the hydrophobicity of the lipid hydrocarbon tails. The greater the saturation and number of carbons in the tail the more hydrophobic the tail region becomes. Data on the transfer of long chain hydrocarbons to water show a linear dependence of the hydrophobic energy on the number of carbon atoms with a prefactor $O(1)$ (Marsh, 1996). For an amphiphilic lipid molecule, reduction in the tail hydrophobic free energy drives clustering of lipid tails and aggregation. The more densely the lipid molecules pack, the less the tails are exposed to water, thus the hydrophobic free energy of a bilayer decreases with decreasing area per molecule, and can be thought of as the attractive component of the total free energy. This leaves the hydration of the headgroup, lipid internal energy, and the coupling between monolayers as the repulsive components. An equilibrium surface density is achieved by minimizing the total free energy with respect to area per molecule (a):

$$\partial_a F_b \sim \gamma_{phob} + \pi_{repul} \quad (2)$$

where $\gamma_{phob} = \partial_a \psi_{phob}$ is simply the hydrophobic free energy surface density and $\pi_{repul} = \partial_a \psi_{hyd} + \partial_a \psi_{int} + \partial_a \psi_{m-m}$ is the repulsive component of the free energy density. Dimensionally, the free energy densities are equivalent to surface pressures: $[\gamma_{phob}] = [\pi_{repul}] = J/m^2 = N{\cdot}m/m^2 = N/m$.

Thermodynamic equilibrium of a lipid membrane can therefore be thought of mechanically as a balance of the positive surface pressure generated by the hydrophobic effect of the tails and the negative pressure arising from lipid repulsive interactions:

$$\gamma_{phob} \sim -\pi_{repul} \quad (3)$$

Using hydrocarbon solubility data, literature calculations for the magnitude of the hydrophobic free energy of lipid plasma membranes is in the range of 30–40 mN/m ($O(1 \times 10^{-20}$ J/nm$^2)$) (Marsh, 1996).

Langmuir monolayers (the primary system of study in this paper) can be equivalently described using the above formalism. The surface free energy of a monolayer contains the lipid internal energy, the hydration energy, and the monolayer–air interaction. Because the tails in the case of a monolayer are free to associate with only the hydrophobic gaseous super-phase, there is no hydrophobic free energy term. A monolayer of lipids spread on an infinite surface would simply expand to vanishing densities, i.e. it will not self-assemble into interacting surface structures. However, using a Langmuir trough the lipid monolayer density can be controlled by exerting a lateral pressure. The monolayer is thermodynamically and mechanically at equilibrium when the lateral pressure exerted by compression (Π_m) matches that of the repulsive internal pressure components:

$$\Pi_m \sim -\pi_{repul} \quad (4)$$

Given that the repulsive free energy components of a lipid monolayer and bilayer are the same, a bilayer monolayer equivalence relationship arises:

$$\gamma_{phob} \sim \Pi_m \quad (5)$$

The lateral surface pressure measured in a Langmuir monolayer is equivalent to the positive compressive pressure experienced by lipids in a lipid membrane because of the hydrophobic effect. The Langmuir monolayer stability experiments are designed to evaluate how lysoPC, oxPAPC, PAPC, and DMPC respond under different external stresses. The two parameters evaluated were monolayer ability to maintain a given surface pressure under constant area conditions ($\Delta\Pi$). and monolayer area loss under constant pressure conditions (A/A_0). When initially prepared, lipids in a Langmuir monolayer are completely surface associated. As the monolayer is compressed, the monolayer surface free energy density increases since lipid repulsive interactions scale directly with density. In all self-assembled membranes, mono- or bi-layered, lipid molecules are free to exchange in and out of the membrane by solubilizing into the surrounding water. Clearly, the energetic cost incurred by doing so is related to the hydrophobic free energy of the lipid tails. In monolayers, when the surface free energy surpasses the hydrophobic free energy ($\Pi_m > \gamma_{phob}$), lipid molecules leave the surface and dissolve into the water subphase. In the context of our experiments, the loss of surface lipids manifests itself as a $\Delta\Pi < 0$ or $A/A_0 < 1$. These monolayer stability criteria, in-turn, allow us to predict the stability of lysoPC and oxPAPC in plasma membranes with respect to solubilizing into the extra cellular fluid.

As shown in Figs. 2 and 3, DMPC remained completely surface associated up to pressures of 35 mN/m. We interpret this result to mean that in the plasma membrane a patch of DMPC would remain membrane associated. lysoPC monolayers showed substantial instability with increasing lateral pressure, indicating that lysoPC solubilizes readily into the subphase, and that the rate as well as the propensity to solubilize scale with surface pressure. oxPAPC shows intermediate surface stability but behaves much more closely to DMPC than to lysoPC.

As mentioned above, the physicochemical basis of Langmuir monolayer stability is lipid hydrophobicity. One direct measurement of hydrophobicity in amphiphiles is the critical micelle concentration. Very hydrophobic lipids have small CMC values while more hydrophilic ones tend to higher CMCs. Fig. 7 shows the CMC data derived from Gibbs adsorption isotherms for lysoPC and oxPAPC. Using Fig. 7C the CMC for oxPAPC is defined to be in the 0.5–1 μM range, while lysoPC shows a much broader range of 0.5–4 μM indicative of a less hydrophobic molecule (Ritacco et al., 2010).

Corroborating our thermodynamic analysis, Fig. 5 shows the rate of solubilization from a model cell membrane is greater for lysoPC than for oxPAPC. Furthermore, as shown in Fig. 6A, when oxidized phospholipids are mixed together in a model cell membrane with nonoxidized phospholipids, lysoPC solubilizes from the membrane more rapidly than other oxidized phospholipids. After ~2000 s, the rate of area loss of a model cell membrane composed of lysoPC and PAPC returns to that of a model membrane without lysoPC regardless of the initial lysoPC concentration. However, model membranes containing oxPAPC instead of lysoPC do not decay to the same base rate for at least 18,000 s, which is likely due to the decreased rate of solubilization of the oxPAPC from the model membrane relative to the rate of solubilization of lysoPC.

In Fig. 10, we outline a model building upon the biological hypothesis of differential oxidized lipid release as well as our surface data. Fig. 10I depicts a membrane patch in mechanical equilibrium with the rest of the cell membrane. The black arrows represent the positive pressure exerted on the membrane, the magnitude of this pressure will be in the range of 30–40 mN/m and, as discussed above, is derived from the hydrophobic effect. The patch remains in equilibrium as long as it is capable of matching the external membrane pressure: $\gamma_{phob}^{membrance} = \gamma_{phob}^{patch}$. Fig. 10II shows our patch undergoing oxidation, whereby the chemical composition of the outer patch leaflet is changed to include not only standard membrane lipids (black) but also lysoPC (red) and oxPAPC (blue) (Cribier et al., 1993). Our model focuses on how the altered chemical structure of the oxidized lipids changes their hydrophobic free energy density and their corresponding propensity to solubilize.

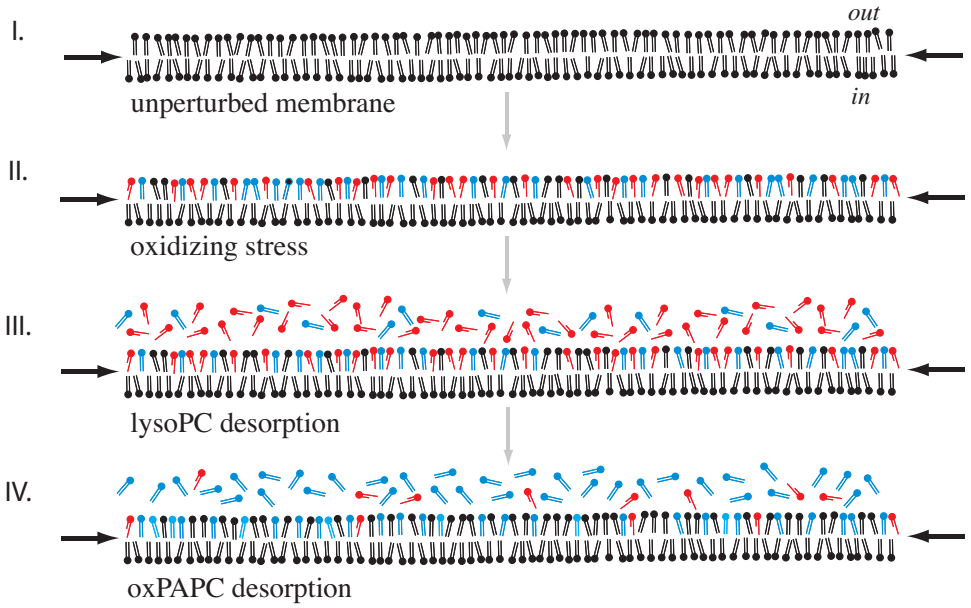

Fig. 10. Differential release model of oxidized phospholipids from the outer leaflet of the lipid bilayer. (I) represents the unperturbed lipid bilayer modeled using a monolayer held at 30 mN/m (indicated by black arrows); such a monolayer undergoes a lipid packing density, and thus hydrophobic free energy density, that is equivalent to that of a bilayer (see main text). PAPC, which is what oxPAPC and lysoPC are believed to originate from, exists in the outer membrane leaflet. When exposed to oxidizing stress, oxidized lipids are generated. In (II) this is represented by lysoPC in red, the oxPAPC species in blue, with black being un-oxidized components of the bilayer. Given lysoPC's low hydrophobicity it desorbs rapidly from the membrane (III) generating a oxPAPC enriched state (IV), which returns to the initial membrane more slowly as oxPAPC desorbs. (For interpretation of the references to color in this figure legend, the reader is referred to the web version of the article.)

Based upon the above stability data, $\gamma_{phob}^{lyso} \ll \gamma_{phob}^{oxPAPC} \leq \gamma_{phob}^{membrance}$, indicating lysoPC is the least stable phospholipid of those probed in a cell membrane. Our kinetic data confirm that lysoPC is the most rapidly solubilized phospholipid, and, in a membrane containing both lysoPC and oxPAPC, will leave the membrane enriched in oxPAPC, which solubilizes at a much slower rate.

This study goes on to explore the role of oxidatively modified phospholipids in vascular leak by demonstrating the opposite and offsetting effects of fragmented phospholipid lysoPC and oxPAPC on endothelial barrier properties. Cell culture experiments show that oxPAPC causes barrier protective effect in the range of concentrations used. These effects are reproduced if endothelial cells are treated with a major oxPAPC compound, PEIPC (data not shown). In contrast, fragmented phospholipid lysoPC failed to induce barrier protective effects and, instead, caused EC barrier compromise in a dose-dependent manner. Importantly, EC barrier dysfunction caused by fragmented phospholipids may be reversed by the introduction of barrier protective oxPAPC concentrations, suggesting an important role of the balance between oxygenated and fragmented lipid components in the control of endothelial permeability.

These data show for the first time the possibility of vascular endothelial barrier control through paracrine signaling by changing the proportion between fragmented (lysoPC) and full length oxygenated phospholipids (oxPAPC), which are present in circulation in physiologic and pathologic conditions. Throughout the period of oxidative stress, both full length oxygenated PAPC products and fragmented phospholipids such as lysoPC are formed. While lysophospholipids are rapidly released from the cell membrane where they are produced, the slower rate of release of full length oxygenated PAPC products into circulation results in the creation of a reservoir of the full-length products in the cell membrane. During the resolution phase of acute lung injury, oxidative stress subsides and we speculate that generation of lysophospholipids is largely decreased due to down regulation of membrane-bound phospholipases, decreased ROS production, and more effective lysophospholipids degradation by PAF-acetyl hydrolase (PAH). Continuing preferred release of lysophospholipids from lipid layers described in this study leads to their clearance from the membranes and efficient degradation by PAH, while full length oxygenated PAPC products (oxPAPC) are more resistant to PAH and stay in surrounding medium for a longer period (V. Bochkov, University of Vienna, personal communication). Finally, later release of full-length oxygenated PAPC products, known to enhance vascular endothelial barrier properties, may be an important mechanism of endothelial barrier restoration during resolution phase of ALI.

Thus, differential release of barrier protective and barrier disruptive products of phospholipid oxidation from cell membranes in injured tissues may create different types of microenvironment at different stages of the inflammatory process in the lungs during ALI, which may contribute to both acute injury phase and later phase of lung vascular endothelial barrier restoration corresponding to ALI recovery phase.

In conclusion, these data demonstrate that: (a) changes in balance between endogenously released oxPAPC species may shift overall lung tissue response from proinflammatory to barrier restoration; and (b) exogenously administered barrier protective oxPAPC formulations may be considered for therapeutic treatment of acute lung injury. These results further support our previous studies that showed improvement of acute lung injury and inflammation induced by lipopolysaccharide or high tidal volume mechanical ventilation by oxPAPC (Nonas et al., 2006).

References

Birukov, K.G., Bochkov, V.N., Birukova, A.A., Kawkitinarong, K., Rios, A., Leitner, A., Verin, A.D., Bokoch, G.M., Leitinger, N., Garcia, J.G.N., 2004. Epoxycyclopentenone-containing oxidized phospholipids restore endothelial barrier function via Cdc42 and Rac. Circulation Research 95, 892–901.

Birukova, A.A., Fu, P., Chatchavalvanich, S., Burdette, D., Oskolkova, O., Bochkov, V.N., Birukov, K.G., 2007. Polar head groups are important for barrier protective effects of osidized phospholipids on pulmonary endothelium. American Journal of Physiology – Lung Cellular and Molecular Physiology 292, L924–L935.

Bochkov, V.N., Oskolkova, O.V., Birukov, K.G., Levonen, A.L., Binder, C.J., Stockl, J., 2010. Generation and biological activities of oxidized phospholipids. Antioxidants and Redox Signalling 12, 1009–1059.
Carpenter, C.T., Price, P.V., Christman, B.B., 1998. Exhaled breath condensate isoprostanes are elevated in patients with acute lung injury or ARDS. Chest 114, 1653–1659.
Cribier, S., Morrot, G., Zachowski, Z., 1993. Dynamics of the membrane lipid phase. Prostaglandins, Leukotrienes and Essential Fatty Acids 48, 27–32.
Feng, S., Brockman, H.L., MacDonald, R.C., 1994. On osmotic-type equations of state for liquid-expanded monolayers of lipids at the Air–Water interface. Langmuir 10, 3188–3194.
Frey, B., Haupt, R., Alms, S., Holzmann, G., Konig, T., Kern, H., Kox, W., Rustow, B., Schlame, M., 2000. Increase in fragmented phosphatidylcholine in blood plasma by oxidative stress. The Journal of Lipid Research 41, 1145–1153.
Giaever, I., Keese, C.R., 1993. A morphological biosensor for mammalian cells. Nature 366, 591–592.
Gopal, Lee, 2001, A., Lee, K.Y.C., 2001. Morphology and collapse transitions in binary phospholipid monolayers. Journal of Physical Chemistry B 105, 10348.
Huber, J., Vales, A., Mitulovic, G., Blumer, M., Schmid, R., Witztum, J.L., Binder, B.R., Leitinger, N., 2002. Oxidized membrane vesicles and blebs from apoptotic cells contain biologically active oxidized phospholipids that induce monocyte–endothelial interactions. Arteriosclerosis, Thrombosis, and Vascular Biology 22, 101–107.
Kadl, A., Bochkov, V.N., Huber, J., Leitinger, N., 2004. Apoptotic cells as sources for biologically active oxidized phospholipids. Antioxidants and Redox Signaling 6, 311–320.
Lang, J.D., McArdle, P.J., O'Reilly, P.J., Matalon, S., 2002. Oxidant-antioxidant balance in acute lung injury. Chest 122, 314S–320S.
Marsh, D., 1996. Lateral pressure in membranes. Biochimica et Biophysica Acta 1286, 183–223.
Montuschi, P., Collins, J.V., Ciabattoni, G., Lazzeri, N., Corradi, M., Kharitonov, S.A., Barnes, P.J., 2000. Exhaled 8-isoprostane as an in vivo biomarker of lung oxidative stress in patients with COPD and healthy smokers. American Journal of Respiratory and Critical Care Medicine 162, 1175–1177.
Munoz, N.M., Meliton, A.Y., Lambertino, A., Boetticher, E., Learoyd, J., Sultan, F., Zhu, X., Cho, W., Leff, A.R., 2006. Transcellular secretion of group V phospholipase A2 from epithelium induces beta 2-integrin-mediated adhesion and synthesis of leukotriene C4 in eosinophils. Journal of Immunology 177, 575–582.
Munoz, N.M., Meliton, A.Y., Meliton, L.N., Dudek, S.M., Leff, A.R., 2009. Secretory group V phospholipase A2 regulates acute lung injury and neutrophilic inflammation caused by LPS in mice. American Journal of Physiology – Lung Cellular and Molecular Physiology 296, L879–L887.
Nonas, S.A., Miller, I., Kawkitinarong, K., Chatchavalvanich, S., Gorshkova, I., Bochkov, V.N., Leitinger, N., Natarajan, V., Garcia, J.G.N., Birukov, K.G., 2006. Oxidized phospholipids reduced vascular leak and inflammation in rat model of acute lung injury. American Journal of Respiratory and Critical Care Medicine 173, 1130–1138.
Oskolkova, O.V., Afonyushkin, T., Preinerstorfer, B., Bicker, W., von Schlieffen, E., Hainzl, E., Demyanets, S., Schabbauer, G., Lindner, W., Tselepis, A.D., Wojta, J., Binder, B.R., Bochkov, V.N., 2010. Oxidized phospholipids are more potent antagonists of lipopolysaccharide than inducers of inflammation. Journal of Immunology 185, 7706–7712.
Pocivavsek, L., Dellsy, R., Kern, A., Johson, S., Lin, B., Lee, K.Y.C., Cerda, E., 2008a. Stress and fold localization in thin elastic membranes. Science 320, 912.
Pocivavsek, L., Frey, S.L., Krishan, K., Gavrilov, K., Ruchala, P., Waring, A.J., Walther, F.J., Dennin, M., Witten, T.A., Lee, K.Y.C., 2008b. Lateral stress relaxation and collapse in lipid monolayers. Soft Matter 4, 2019.
Qiao, J., Huang, F., Naikawadi, R.P., Kim, K.S., Said, T., Lum, H., 2006. Lysophosphatidylcholine impairs endothelial barrier function through the G protein-coupled receptor GPR4. American Journal of Physiology – Lung Cellular and Molecular Physiology 291, L91–L101.
Quinlan, G.J., Lamb, N.J., Evans, T.W., Gutteridge, J.M., 1996. Plasma fatty acid changes and increased lipid peroxidation in patients with adult respiratory distress syndrome. Critical Care Medicine 24, 214–246.
Ritacco, H., Langevin, D., Diamant, H., Andelman, D., 2010. Dynamic surface tension of aqueous solutions of ionic surfactants: role of electrostatics. Langmuir 27, 1009–1014.
Shanely, R.A., Zergeroglu, M.A., Lennon, S.L., Sugiura, R., Yimlamai, T., Enns, D., Belcastro, A., Powers, S.K., 2002. Mechanical ventilation-induced diaphragmatic atrophy is associated with oxidative injury and increased proteolytic activity. American Journal of Respiratory and Critical Care Medicine 166, 1369–1374.
Starosta, V., Wu, T., Zimman, A., Pham, D., Tian, X., Oskolkova, O., Bochkov, V., Berliner, J., Birukova, A., Birukov, K., 2012. Differential regulation of endothelial cell permeability by high and low doses of oxidized 1-palmitoyl-2-arachidonyl-sn-glycero-3-phosphocholine. American Journal of Respiratory Cell and Molecular Biology 46, 331–341.
Subbanagounder, G., Leitinger, N., Schwenke, D.C., Wong, J.W., Lee, H., Rizza, C., Watson, A.D., Faull, K.F., Fogelman, A.M., Berliner, J.A., 2000. Determinants of bioactivity of oxidized phospholipids. Specific oxidized fatty acyl groups at the sn-2 position. Arteriosclerosis, Thrombosis, and Vascular Biology 20, 2248–2254.
Tiruppathi, C., Malik, A.B., Del Vecchio, P.J., Keese, C.R., Giaever, I., 1992. Electrical method for detection of endothelial cell shape change in real time: assessment of endothelial barrier function. Proceedings of the National Academy of Sciences of the United States of America 89, 7919–7923.
Van Lenten, B.J., Wagner, A.C., Navab, M., Anantharamaiah, G.M., Hui, E.K., Nayak, D.P., Fogelman, A.M., 2004. D-4F, an apolipoprotein A-I mimetic peptide, inhibits the inflammatory response induced by influenza A infection of human type II pneumocytes. Circulation 110, 3252–3258.
Watson, A.D., Leitinger, N., Navab, M., Faull, K.F., Hörkkö, S., Witztum, J.L., Palinski, W., Schwenke, D., Salomon, R.G., Sha, W., Subbanagounder, G., Fogelman, A.M., Berliner, J.A., 1997. Structural identification by mass spectrometry of oxidized phospholipids in minimally oxidized low density lipoprotein that induce monocyte/endothelial interactions and evidence for their presence in vivo. Journal of Biological Chemistry 272, 13597–13607.
Wolfe, D.H., Brockman, H.L., 1988. Regulation of the surface pressure of lipid monolayers and bilayers by the activity of water: derivation and application of an equation of state. Proceedings of the National Academy of Sciences of the United States of America 85, 4285–4289.
Yan, S., Chai, H., Wang, H., Yang, H., Nan, B., Yao, Q., Chen, C., 2005. Effects of lysophosphatidylcholine on monolayer cell permeability of human coronary artery endothelial cells. Surgery 138, 464–473.